antenna for maximum radiated power (0 dB value). The antenna shows very symmetrical patterns. The 3 dB and 10 dB mainbeam widths are 22° and 38°, respectively. The maxima of the sidelobes are −14 dB at ±40°. Measured and simulated data (dash-dotted line in Fig. 3, [12]) show very good agreement. The measurement is limited to ±60° due to the measurement setup. The cross-polarization isolation of the triple patch antenna is better than −30 dB at 0°.

V. Conclusion

Planar microstrip antennas for operation for 77 GHz have been realized and tested. For the fabrication of the antennas new technology steps have been developed which are compatible to standard GaAs processing techniques. The antenna patches are suspended on thin freestanding SiN_x membranes on GaAs substrate. The patches are coupled through an aperture in the ground metallization of the feeding microstrip circuit. For the design the method of moments in spectral domain has been applied. The triple patch antennas exhibit symmetrical radiation patterns with a 10 dB mainbeam width of 38°. Very good correspondence between measurement and simulation has been observed. To the authors knowledge the demonstrated results represent the first data for aperture-coupled millimeter-wave patch antennas on thin membranes fabricated on GaAs.

Acknowledgment

The authors would like to thank S. Heuthe and H. Mietz for technological support and K.-E. Schmegner and T. Schmidt for advice and help concerning the design of the test-fixtures and the mounting of the antennas. Special thanks also to R. Schneider and H. Rudolf for their assistance during the antenna pattern measurements.

References

[1] M. J. Vaughan, K. Y. Hur, and R. C. Compton, "Improvement of microstrip patch antenna radiation patterns," *IEEE Trans. Antennas Propagat.*, vol. 42, pp. 882–885, June 1994.

[2] G. M. Rebeiz, personal communications.

[3] ——, "Millimeter-wave and terahertz integrated circuit antennas," *Proc. IEEE*, vol. 80, pp. 1748–1770, Nov. 1992.

[4] C.-Y. Chi and G. M. Rebeiz, "Planar microwave and millimeter-wave lumped elements and coupled-line filters using micro-machining techniques," *IEEE Trans. Microwave Theory Tech.*, vol. 43, no. 4, pp. 730–738, Apr. 1995.

[5] T. M. Weller, L. P. Katehi, and G. M. Rebeiz, "A 250-GHz microshield bandpass filter," *IEEE Microwave Guided Wave Lett.*, vol. 5, no. 5, pp. 153–155, May 1995.

[6] W. Y. Ali-Ahmad, W. L. Bishop, T. W. Crowe, and G. M. Rebeiz, "An 86–106 GHz quasiintegrated low-noise Schottky receiver," *IEEE Trans. Microwave Theory Tech.*, vol. 41, no. 4, pp. 558–564, Apr. 1993.

[7] K. R. Carver and J. W. Mink, "Microstrip antenna technology," *IEEE Trans. Antennas Propagat.*, vol. AP-29, pp. 2–24, Jan. 1981.

[8] D. M. Pozar, "A reciprocity method of analysis for printed slot and slot-coupled microstrip antennas," *IEEE Trans. Antennas Propagat.*, vol. AP-34, pp. 1439–1446, Dec. 1986.

[9] F. Rostan, E. Heidrich, and W. Wiesbeck, "Design of aperture-coupled patch antenna arrays with multiple dielectric layers," in *Proc. 23rd European Microwave Conf. EuMC'93*, Madrid, Spain, Sept. 6–9, 1993, pp. 917–919.

[10] A. Kiermasz, S. Harrington, J. Bhardwaj, and A. McQuarrie, "Stress control during PECVD of silicon nitride films using a new technique," S.T.S. Tech. Paper, Bristol, U.K., 1987.

[11] W. A. Claassen, W. G. Valkenburg, M. F. Willemsen, and W. M. v.d. Wijgert, "Influence of deposition temperature, gas pressure, gas phase composition, and RF frequency on composition and mechanical stress of plasma silicon nitride layers," *J. Electrochem. Soc.*, vol. 132, pp. 893–898, Apr. 1985.

[12] Mikavica and A. Nesic, "CAD for linear and planar antenna arrays of various radiating elements," *Software and User's Manual.* Norwood, MA: Artech House, 1992.

Application of the Spatial Finite-Difference and Temporal Differential (SFDTD) Formulation to Cylindrical Structure Problems

Alan Ming Keung Chan and Zhizhang Chen

***Abstract*—The recently developed spatial finite-difference and temporal differential (SFDTD) approach is extended to dielectric loaded cylindrical environments. Although the method is developed differently, its resultant formulation can be directly obtained from the corresponding finite-difference time-domain (FD-TD) method. Good agreements between the SFDTD and reference results are obtained for different configurations of dielectric loaded cylindrical structures. As a result, the SFDTD approach is shown to be generally effective and robust for resonant structures.**

I. Introduction

Cylindrical cavities, especially in dielectric-loaded structures, have been widely used in many microwave applications such as filter, oscillator, and dielectric measurement [1]–[4]. Characterization of these structures for applications in microwave circuits is required. Different approaches for the structures consisting of transmission media and their boundaries have been used. In the past, analytical methods, such as spectral domain method and mode matching technique, were applied; however, the methods require the specific structures and cannot be applied to the problems with arbitrary geometry. Furthermore, the realistic features such as finite metallization thickness, mounting groove, and irregularities caused during manufacturing, cannot be easily accounted for. Therefore, very accurate characterization numerical techniques are essential to model the problems.

Numerical techniques such as the finite element method (FEM), the method of moment (MoM), the boundary element method (BEM) have evolved in the last two decades. Recent advances in modeling concepts and computer technology have expanded the scope, accuracy and speed of these methods. Typically, time-domain techniques such as the finite-difference time-domain (FD-TD) method and the transmission line matrix (TLM) method have received growing attention due to the simplicity and flexibility of their algorithms. Programs based on these techniques can be applied to solve problems with structures that the analytical approaches cannot deal with. However, when these time-domain methods are applied to resonant structures, they encounter certain difficulties. For example, for a high-Q structure, long iteration may be required. Also, resonant modes may be missed due to the placement of excitation or output points at the null field points of the modes.

Recently, a numerical method which circumvents the problems mentioned above is developed and applied to homogeneous rectangu-

Manuscript received November 10, 1995; revised May 24, 1996. This work was supported by the Natural Science and Engineering Research Council of Canada.

The authors are with the Department of Electrical Engineering, Technical University of Nova Scotia, Halifax, Nova Scotia B3J 2X4, Canada.

Publisher Item Identifier S 0018-9480(96)06398-3.

lar structures [5]. The method is based on the spatial finite-difference and temporal differential (SFDTD) formulation of Maxwell's equations in which the problem is formulated in time domain while the solutions are obtained in a manner very much similar the frequency-domain methods. In this paper, the SFDTD approach is extended to inhomogeneous cylindrical environments. The structures considered in this paper for testing the effectiveness and accuracy of the SFDTD method include: 1) the cavity loaded by dielectric at the base, 2) the cavity loaded by the dielectric button, and 3) the shielded dielectric resonator. The numerical results are then compared with analytical solutions and the results obtained with other techniques.

II. Theory

For simplicity, a stationary, lossless and sourceless medium is assumed with the note that the principle can be easily applied to other cases. Maxwell's equations in cylindrical coordinate system (r, θ, z) can then be expressed as a system of six scalar equations. For example, for Ez, one can have

$$\frac{\partial E_z}{\partial t} = \frac{1}{r}\left[\frac{\partial (rH_\theta)}{\partial r} - \frac{\partial H_r}{\partial \theta}\right]. \tag{1}$$

By following Yee's grid arrangement for discretization of the spatial domain [14] while retaining the time-domain differentials in Maxwell's equations, the SFDTD formulation can be obtained. For example, as in (2) shown at the bottom of the page, where a spaced cylindrical grid of points is defined as

$$(t, i_r\delta r, i_\theta\delta\theta, i_z\delta z) = (t, i_r, i_\theta, i_z) \tag{3}$$

and any function of discrete space and *continuous* time as

$$F(t, i_r\delta r, i_\theta\delta\theta, i_z\delta z) = F(t, i_r, i_\theta, i_z). \tag{4}$$

Here t is the notation for time while δr, $\delta\theta$, and δz are the space increments along the r, θ, and z directions, respectively. $r_{i_r} = i_r\delta r$. i_r, i_θ, and i_z are integers. r_0 is the averaging distance of r_i and r_{i+1}, the radius of the two neighboring nodes. The equations for other components can be found in a similar way.

For a specific type of waves, the equations can be simplified. For instance, for TM_0 (to z-axis) waves ($H_r = H_z = 0$, $E_\theta = 0$), one can have

$$\frac{\partial E_z\left(t, i_r, i_z + \frac{1}{2}\right)}{\partial t} = \frac{1}{r_0}\left[\frac{r_2 H_\theta\left(t, i_r + \frac{1}{2}, i_z + \frac{1}{2}\right) - r_1 H_\theta\left(t, i_r - \frac{1}{2}, i_z + \frac{1}{2}\right)}{\varepsilon\delta r}\right]. \tag{5}$$

For TE_0 (to z-axis) waves ($E_r = E_z = 0$, $H_\theta = 0$), a similar equation can be obtained.

The main difference between the above formulation and the conventional finite-difference time-domain scheme lies in the fact that in the FD-TD scheme [7], both temporal differentials and the spatial derivatives in Maxwell's equations are replaced by the corresponding finite differences. With this method, only the spatial derivatives in Maxwell's equations are replaced while the temporal differentials remain unchanged.

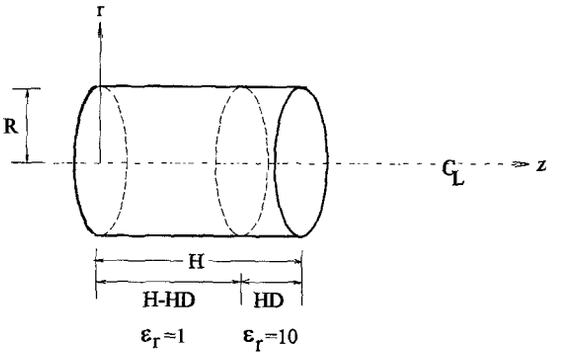

Fig. 1. Cylindrical cavity with radius R and height H, and dielectric medium with thickness HD and relative permittivity ε_r.

By carrying out the above SFDTD process for Maxwell's equations, one can obtain the SFDTD form of Maxwell's equations in the cylindrical coordinates in a matrix form

$$\frac{d\mathbf{H}}{dt} = \mathbf{D}_1\mathbf{E} \tag{6}$$

$$\frac{d\mathbf{E}}{dt} = \mathbf{D}_2\mathbf{H} \tag{7}$$

where $\mathbf{D}_1$ is a $N_h \times N_e$ matrix and $\mathbf{D}_2$ is a $N_e \times N_h$ matrix. N_h is the total number of H nodes while N_e is the total number of E nodes.

Taking temporal derivative on (6) and then substituting (7) into (6), one can obtain

$$\frac{d^2\mathbf{H}}{dt^2} = \mathbf{D}_1\mathbf{D}_2\mathbf{H} = \mathbf{D}_{12}\mathbf{H} \tag{8}$$

where $\mathbf{D}_{12} = \mathbf{D}_1 \cdot \mathbf{D}_2$ is a $N_h \times N_h$ sparse matrix.

Note that $\mathbf{D}_1$ and $\mathbf{D}_2$ can actually be extracted from the FD-TD formulations used in [7] by simply discarding the terms resulting from the temporal finite-differences.

Let $\mathbf{D}$ be the $N_h \times N_h$ diagonal matrix with its diagonal elements λ_j $(j = 1, 2, \ldots, N_h)$ being the eigenvalues of $\mathbf{D}_{12}$ and let $\mathbf{Y}$ be the $N_h \times N_h$ matrix whose columns are the eigenvectors y_j of $\mathbf{D}_{12}$. Then, the solution of (8) leads to

$$\begin{aligned}\mathbf{H} &= \mathbf{Y}e^{\sqrt{\mathbf{D}}t}\mathbf{a} \\ &= a_1 e^{\sqrt{\lambda_1}t}y_1 + a_2 e^{\sqrt{\lambda_2}t}y_2 + \cdots + a_{N_h}e^{\sqrt{\lambda_{N_h}}t}y_{N_h}\end{aligned} \tag{9}$$

where the constant vector $\mathbf{a} = [a_1, a_2, \ldots, a_{N_h}]$ is determined by the initial condition of $\mathbf{H}$, i.e. values of $\mathbf{H}$ at $t = 0$.

As can be seen now, finding the numerical solution is now becoming finding the eigenvalues λ_j and eigenvectors y_j of $\mathbf{D}_{12}$ (which is sparse). For resonant structures, $\sqrt{\lambda_j}$ obviously corresponds to resonant frequencies while y_j is the eigenfield distributions.

Similar procedures can be performed for $\mathbf{E}$ by taking temporal derivative on (7) and substituting (6) into (7). The result is to find the eigensolution of a $N_e \times N_e$ matrix $\mathbf{D}_{12}$. Obviously, either $\mathbf{E}$ and $\mathbf{H}$ can be chosen for solutions. However, in term of computation cost, the choice for selecting $\mathbf{E}$ or $\mathbf{H}$ for solutions is preferred by the size of $\mathbf{D}_{12}$. If $N_e < N_h$, choose $\mathbf{E}$. If $N_e > N_h$, choose $\mathbf{H}$. In this way, a smaller size of $\mathbf{D}_{12}$ can be obtained; therefore, computation

$$\frac{\partial E_z\left(t, i_r, i_\theta, i_z + \frac{1}{2}\right)}{\partial t} = \frac{1}{r_0}\left[\frac{r_{i_r+\frac{1}{2}}H_\theta\left(t, i_r + \frac{1}{2}, i_\theta, i_z + \frac{1}{2}\right) - r_{i_r-\frac{1}{2}}H_\theta\left(t, i_r - \frac{1}{2}, i_\theta, i_z + \frac{1}{2}\right)}{\varepsilon\delta r} - \frac{H_r\left(t, i_r, i_\theta + \frac{1}{2}, i_z + \frac{1}{2}\right) - H_r\left(t, i_r, i_\theta - \frac{1}{2}, i_z + \frac{1}{2}\right)}{\varepsilon\delta\theta}\right] \tag{2}$$

TABLE I
COMPARISON OF THE RESONANT FREQUENCIES FOR THE CAVITY LOADED BY DIELECTRIC AT ONE END

Modes	Theoretical frequency (GHz)	FD-TD DFT [7] frequency (GHz)	SFDTD frequency (GHz)	% difference between SFDTD results and	
				DFT	theoretical
TM_{011}	5.640	5.64	5.652	0.21	0.21
TE_{01}	8.847	8.84	8.879	0.44	0.36
TM_{021}	9.497	9.486	9.494	0.08	0.03
TM_{012}	11.181	11.17	11.245	0.67	0.57
TE_{02}	12.974	12.96	12.984	0.18	0.08

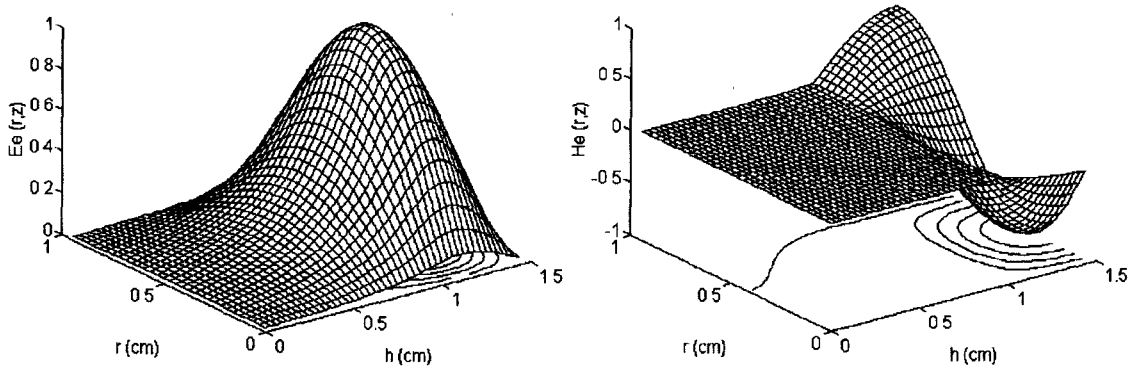

(a) (b)

Fig. 2. (a) E_θ distributions of TE_{01} and (b) H_θ distributions of TM_{021} for the cylindrical cavity loaded with dielectric at one end considered in Table I.

count is reduced. For example, $\mathbf{H}$ is chosen for TM_0 while $\mathbf{E}$ is chosen for TE_0. Once $\mathbf{H}$ (or $\mathbf{E}$) are obtained, the $\mathbf{E}$ (or $\mathbf{H}$) can be found from (6) and (7).

It is worth mentioning here that although the principle applied here is the same as that in [5], the SFDTD approach here are formulated in an inhomogeneous cylindrical environments. The coefficients of $\mathbf{D}_{12}$ take into account of the inhomogeneity in cylindrical coordinates which include $1/r$ term shown in (5).

III. Numerical Results

In order to test the effectiveness and accuracy of the SFDTD method in an inhomogeneous cylindrical environment, a computer code was written. The first part of the code is to generate the matrix elements $\mathbf{D}_{12}$ from the FD-TD formulation [7]. The second part is to perform the transformation which allows computation of the lowest eigenvalues using the power method as described in [5]. These lowest eigenvalues corresponds to the dominant modes. The third part is to execute the sparsity-based algorithm to obtain the eigenvalues and eigenvectors. In our case, the built-in functions in MATLAB were used and thus, the programming time is much reduced and the computer code is much simplified. The computation time for the following examples is less than five minutes in all the cases on a Pentium 100 MHz PC.

A. Cylindrical Cavity Loaded by a Dielectric Medium at its End

The first example is a cylindrical cavity loaded by a dielectric medium at its end. The parameters are radius $R = 1$ cm, height $H = 1.5$ cm, thickness of the dielectric $HD = 0.5$ cm and relative permittivity $\varepsilon_r = 10$ (Fig. 1). A 48 by 32 grid (h by r) is used to calculate a few dominant resonant frequencies of the TM_0 and TE_0 mode. The numerical results are shown in Table I. For all the TM_0 and TE_0 modes, the results by SFDTD are very close to the theoretical results. The percentage difference is less than 1%. The corresponding eigenfield distributions of the resonant modes are obtained directly by the present method. The field distributions of TE_0 mode and TM_0 modes are shown in Fig. 2. Since the dielectric region ($\varepsilon_r = 10$) is located at the end of the cylindrical cavity, the field has higher intensity in this region as expected.

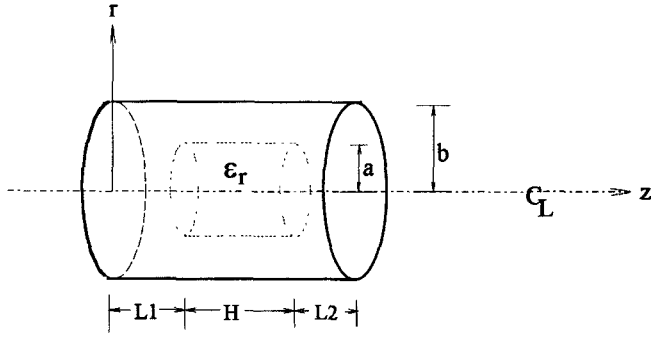

Fig. 3. Cylindrical cavity with radius b, and loaded by a dielectric button with height H, radius a, and relative permittivity ε_r.

B. Cylindrical Cavity Loaded by a Button

The next example is the cylindrical cavity loaded by a dielectric button. The parameters are radius $a = 0.8636$ cm, $b = 1.295$ cm, height $H = 0.762$, $L1 = L2 = 0.381$ cm, and $\varepsilon_r = 35.74$, as shown in Fig. 3. A 14 by 14 grid (h by r) is used for discretization. The results are shown in Table II. TE mode field distribution is shown in Fig. 4(a) and its corresponding contour plot is shown in Fig 4(b). It is symmetric about z-axis since $L1$ and $L2$ are of the same length. However, along r-direction, the field is more concentrated near the center line (z-axis) due to high relative permittivity of the region.

TABLE II
COMPARISON OF THE RESONANT FREQUENCIES FOR THE CAVITY LOADED BY A DIELECTRIC BUTTON

Mode	MM GHz [12]	FEM GHz [13]	FDTD GHz [12]	FDTD general mesh(GHz) [6]	FDTD BOM(GHz) [6]	SFDTD (GHz)
TE_0	3.44	3.51	3.53	3.44	3.46	3.435

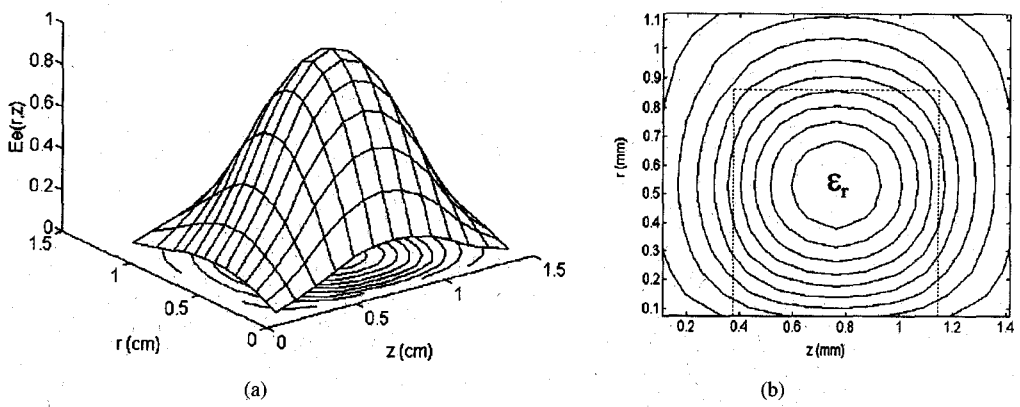

(a) (b)

Fig. 4. (a) Field E_θ distributions and (b) contour plot of TE_0 mode for the cylindrical cavity loaded by dielectric button considered in Table II.

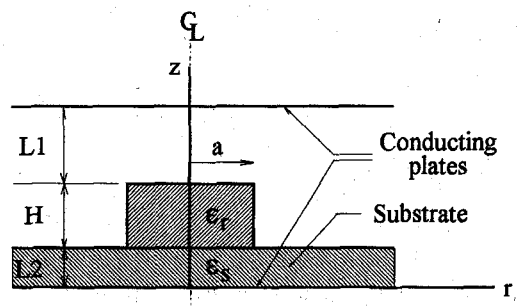

Fig. 5. The shielded dielectric resonator of radius a, height H and dielectric relative permittivity ε_r, and relative substrate permittivity ε_s.

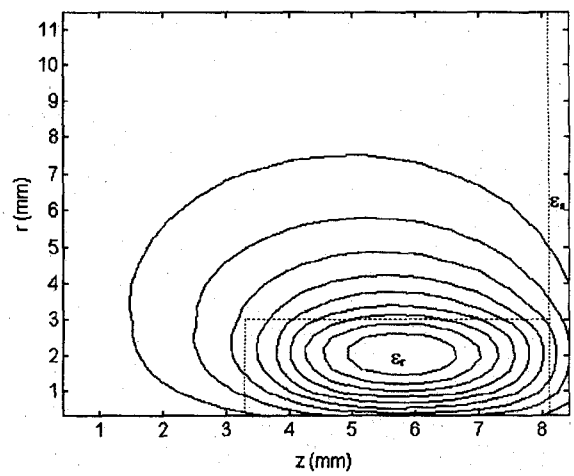

Fig. 6. Contour plot corresponding to field E_θ distributions of $TE_{01\delta}$ mode for the shielded dielectric resonator considered in case (I) in Table III(a).

C. The Shielded Dielectric Resonator

The last example is the shielded dielectric resonator, with variables radius a, length H, $L1$, $L2$, dielectric relative permittivity ε_r and relative substrate permittivity ε_s, shown in Fig. 5. A 20 by 24 grid (h by r) is used for discretization with the proposed method, in comparison with the space mesh of 31 by 47 used with the FD-TD coupled with the DFT method [7]. As the finite-difference method requires a closed boundary, a null field condition at an appropriate distance from the axis has been imposed. This can be justified by the high dielectric permittivity of the resonator where most electromagnetic energy is concentrated. The compromise between the distance and a moderate number of mesh grids has been achieved with a distance equal to three times of the radius of the dielectric resonator [7].

Table III(a) shows comparisons among our results and both the DFT methods and measured results. The percentage difference is generally less than 1%. The contour plot of the field for case i) is shown in Fig. 6. It can be seen that the field is concentrated on the lower part which corresponds to the high relative permittivity region ($\varepsilon_r = 36.3$). On the other hand, since there is a substrate located on the right-hand side having relative substrate permittivity ($\varepsilon_s = 9.25$), the field distribution is not symmetric with respect to z-axis. As a result, there is a small concentration on the right-hand side.

A comparison is also made with the rigorous methods and improved dielectric waveguide model (IDWM) [4] but with different sizes. Again, the space mesh of 20 by 24 grid is used with the proposed method. The results are shown in Table III(b) and Fig. 7. The percentage errors are found to be the less than 1%. Note here that the rigorous methods only served as reference techniques. They are so complicated that their uses in practical design becomes almost prohibitive.

IV. CONCLUSION

The SFDTD method has been applied in the cylindrical environments. The results obtained agree very well with the theoretical or experimental results. The discrepancies are generally less than 2%. Whenever the analytical solutions are available, the errors of the present method are less than 1%. These have demonstrated the effectiveness of the SFDTD in an inhomogeneous cylindrical environment for resonant structures.

TABLE III
COMPARISON OF THE RESONANT FREQUENCIES FOR (a) $TE_{01\delta}$ MODE FOR THE SHIELDED DIELECTRIC RESONATOR AND (b) COMPARISON OF THE RESONANT FREQUENCIES FOR $TE_{01\delta}$ MODE FOR THE SHIELDED DIELECTRIC RESONATOR

Case	εr	εs	a	H	L1	L2	Resonant frequency(GHz) Measured DFT	SFDTD	[7]	% difference between SFDTD and Measured DFT	
i	36.3	9.25	3.03	4.22	3.979	0.7005	8.27	8.25	8.246	0.29	0.05
ii	36.3	9.25	3.015	3.04	5.138	0.6992	9.09	9.04	9.019	0.78	0.23
iii	36.3	9.25	3.01	2.14	6.056	0.6998	10.20	10.12	10.034	1.62	0.85

(a)

εr	εs	a	H	L1	L2	Resonant frequency(GHz) Rigorous DWM[8]	Improved Theory SFDTD		% difference between SFDTD and Rigorous Improved Theory DWM	
34.19	9.6	7.49	7.48	0.72	0.70	4.35[9]	4.34	4.33	0.46	0.23
36.2	1.0	2.03	5.15	2.93	2.93	10.50[1]	10.73	10.57	0.67	1.89

(b)

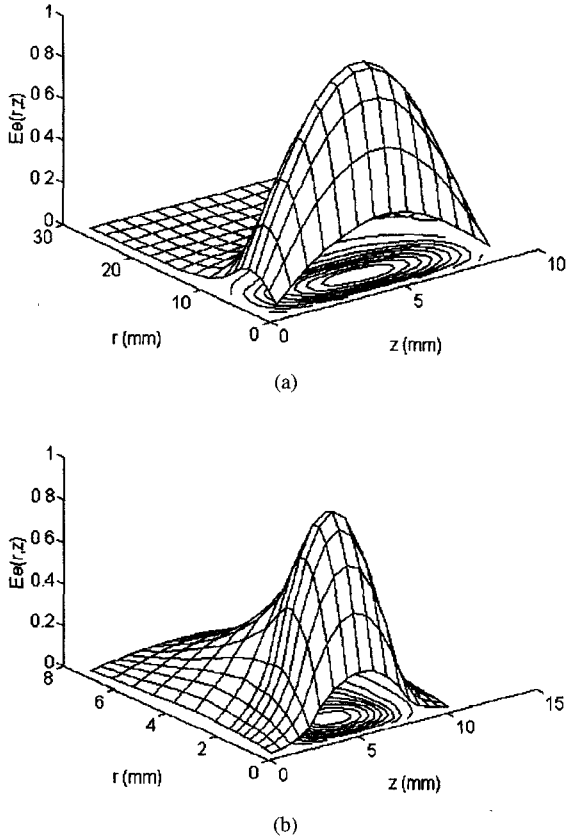

Fig. 7. Field E_θ distributions of $TE_{01\delta}$ mode for the shielded dielectric resonator considered in Table III(b).

The implementation of this technique is relative simple and easy as all the matrix elements can be directly obtained from the conventional FD-TD method and many sparsity-based eigenvalue solvers can be found commercially or in public domains. In other words, an alternative approach of using FD-TD is presented where resonant frequency and mode distribution can be solved directly rather than following the conventional path: direct simulation and then Fourier transform. It avoids the possibility of missing of the modes due to the placement of excitation and output points at the null fields of the modes.

REFERENCES

[1] D. Kajfez and P. Guillon, *Dielectric Resonators*. Norwood, MA: Artech House, 1986.
[2] S. J. Fiedziuszko, "Dual-mode dielectric resonator loaded cavity filters," *IEEE Trans. Microwave Theory Tech.*, vol. MTT-30, pp. 1311–1316, Sept. 1982.
[3] K. A. Zaki, C. Chen, and A. E. Atia, "Canonical and longitudinal dual-mode dielectric resonator filters without iris," *IEEE Trans. Microwave Theory Tech.*, vol. MTT-35, pp. 1130–1135, Dec. 1987.
[4] V. Madrangeas, M. Aubourg, P. Guillon, S. Vigneron, and B. Theron, "Analysis and realization of *L*-band dielectric resonator microwave filters," *IEEE Trans. Microwave Theory Tech.*, vol. 40, pp. 120–127, Jan. 1992.
[5] Z. Chen and A. M. Chan, "A new approach for analysis of resonant structures based on the spatial finite-difference and temporal differential formulation," *IEEE Trans. Microwave Theory Tech.*, vol. 44, no. 4, pp. 631–635, Apr. 1996.
[6] L. Zhao, S. T. Lin, and R. G. Carter, "The influence of boundary conditions on resonant frequencies of cavities in 3-D FDTD algorithm using nonorthogonal coordinates," *IEEE Trans. Microwave Theory Tech.*, vol. 30, pp. 3570–3573, Sept. 1994.
[7] A. Navarro, M. J. Nunez, and E. Martin, "Study of modes in dielectric resonators by a finite difference time-domain method coupled with the discrete Fourier transform," *IEEE Trans. Microwave Theory Tech.*, vol. 39, pp. 14–17, Jan. 1991.
[8] R. K. Mongia, "Resonant frequency of cylindrical dielectric resonator placed in an MIC environment," *IEEE Trans. Microwave Theory Tech.*, vol. 38, no. 6, pp. 802–804, June 1990.
[9] S. Maj and J. W. Modelski, "Application of a dielectric resonator on microstrip line for a measurement of complex permittivity," in *IEEE MTT-S Int. Microwave Symp. Dig.*, 1984, pp. 525–527.
[10] M. Jaworski and M. W. Pospieszalski, "An accurate solution of the dielectric resonator problem," *IEEE Trans. Microwave Theory Tech.*, vol. MTT-27, pp. 639–644, July 1979.
[11] A. Navarro, M. J. Nunez, and E. Martin, "Finite difference time domain FFT method applied to axially symmetrical electromagnetic resonant devices," *Proc. IEE*, vol. 137, pt. H, no. 3, pp. 193–196, 1990.
[12] P. H. Harms, J. F. Lee, and R. Mittra, "A study of the nonorthogonal FDTD method versus the conventional FDTD technique for computing resonant frequencies of cylindrical cavities," *IEEE Trans. Microwave Theory Tech.*, vol. 40, pp. 741–746, Apr. 1992.

[13] D. H. Choi and W. J. R. Hoefer, "The finite-difference time-domain method and its application to eigenvalue problems," *IEEE Trans. Microwave Theory Tech.*, vol. MTT-34, pp. 1464–1470, Dec. 1986.
[14] K. S. Yee, "Numerical solution of initial boundary value problems involving Maxwell's equations in isotropic media," *IEEE Trans. Antennas Propagat.*, vol. AP-14, no. 3, pp. 302–307, May 1966.

Analysis of a Double Step Microstrip Discontinuity in the Substrate Using the 3-D-FDTD Method

Joong Chang Chun and Wee Sang Park

***Abstract*—The finite-difference time-domain (FDTD) method has been applied to the analysis of a double step microstrip discontinuity having thickness changes in the longitudinal direction. The discontinuity occurs in patch antenna feeds or interconnections between microwave planar circuit modules. The simulation results are compared with those computed by HFSS to show a good agreement. An equivalent circuit for the double step discontinuity is developed from the scattering parameters computed by the FDTD method.**

I. Introduction

The planar microwave circuits, microwave integrated circuit (MIC) and monolithic microwave integrated circuit (MMIC), are playing an important role in the development of mobile and satellite communication systems. Among the various forms of planar transmission lines the microstrip line is used most commonly because of its simple structure and extensive research results obtained experimentally or theoretically [1]. Therefore, an accurate analysis of the discontinuities such as step-in-width, open end, gap, bend, T-junction, cross-junction, slit, and slot is essential to the circuit design of filters, matching circuits, transitions, and interconnections [2]. Recently, some microwave applications of transitions or interconnections between two substrates with different permittivities or different thicknesses were reported in [3] and [4], while in the area of optical integrated circuits the discontinuities of permittivity or height have been analyzed by many researchers [5]–[7]. From this point of view, we are interested in the microstrip discontinuities which have changes in the substrate height along the direction of wave propagation.

In this paper, a microstrip discontinuity due to the change of substrate height is analyzed by means of the three-dimensional (3-D) finite-difference time-domain (FDTD) method. The FDTD method, first proposed by Yee [8], is widely used nowadays in the analysis of microstrip discontinuities with the development of computer hardware technology. This method has several advantages in the flexibility of modeling discontinuities and its simplicity in the computer program implementation of Maxwell equations [9]. But no perfect boundary condition for the FDTD method has been developed as yet. Also this method requires large computer resources, which demand proper choice of mesh parameters for computation. The discontinuities for a two-port microstrip line bear various forms such as the changes in the substrate height and permittivity as well as in the strip width. The discontinuity treated in this work is a double step in the substrate height with a uniform strip width and a constant permittivity.

Manuscript received December 1, 1995; revised May 24, 1996. This work was supported by the Agency of Defense Development and Ministry of the Republic of Korea.

J. C. Chun is with the Radio Communications Research Laboratory of Korea Telecom, Seoul, Korea.

W. S. Park is with the Microwave Application Research Center, Department of Electronic and Electrical Engineering, Pohang University of Science and Technology, Pohang, Korea.

Publisher Item Identifier S 0018-9480(96)06392-2.

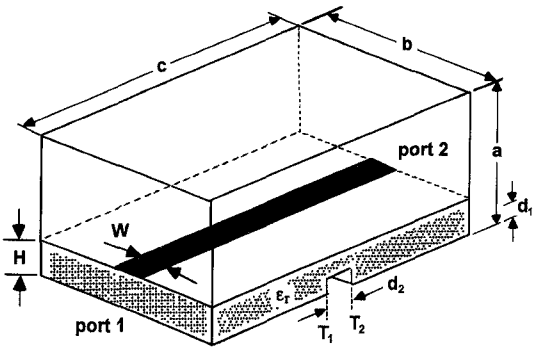

Fig. 1. Perspective view of a microstrip double step discontinuity in the substrate. $a = 5H$, $b = 4W$, $W = 0.593$ mm, $\epsilon_r = 10.2$, $H = 0.635$mm, $d_1 = 0.397$mm, and $d_2 = 0.700$mm.

II. Analysis Method

The FDTD method is well formulated for the analysis of microstrip circuits in several papers [10]–[12]. But the method can be improved by using an excitation pulse whose field configuration is similar to that of the dominant mode of the microstrip line. The excitation pulse used in this research is composed of a quasi-static electric field in the cross section and the time variation of Gaussian function as follows:

$$E_x(t) = e_{x0} e^{-(t-t_0)^2/T^2} \tag{1}$$

$$E_y(t) = e_{y0} e^{-(t-t_0)^2/T^2} \tag{2}$$

where e_{x0} and e_{y0} represent x- and y- components of the quasi-static electric field in the source plane, respectively. The quasi-static field can be easily calculated by the finite difference method [13], and it contains much less components of the higher order modes than the uniformly distributed field under the metal strip [10], [11]. Thus using the quasi-static field yields more stable numerical result.

The propagation constant β and the effective dielectric constant ϵ_{reff} can be calculated from the ratio of the electric fields taken at two nodes a certain distance apart from each other as explained in [10]. But the characteristic impedance Z_0 should be calculated carefully because the electric and magnetic nodes are placed off in space by one half of the space step, and the evaluation of field components is made also at alternate half-time steps. Thus a phase correction factor in the form of an exponent as in (3) has to be included in the usual formula [10]

$$Z_0 = \frac{V(f)}{I(f)} e^{-j\omega\Delta t/2 + j\beta\Delta z/2} \tag{3}$$

where $V(f)$ is the line integral of the electric field under the center of the strip, and $I(f)$ is the loop integral of the magnetic field around the metal strip. For the absorbing boundary condition, the time-space extrapolation method [14] applied to the super-absorbing boundary condition [15] is used.

As a preparatory procedure for the S-parameter calculation of a microstrip discontinuity, an analysis of the corresponding uniform